J Ind Microbiol Biotechnol (2012) 39:649–654
DOI 10.1007/s10295-011-1056-y

METABOLIC ENGINEERING AND SYNTHETIC BIOLOGY

Effect of modified glucose catabolism on xanthan production in *Xanthomonas oryzae* pv. *oryzae*

Se-Gul Jang · Byoung-Moo Lee · Jae-Yong Cho

Received: 19 June 2011 / Accepted: 28 October 2011 / Published online: 11 November 2011

Abstract In this study, the glucose 6-phosphate dehydrogenase gene (XOO2314) was inactivated in order to modulate the intracellular glucose 6-phosphate, and its effects on xanthan production in a wild-type strain of *Xanthomonas oryzae* were evaluated. The intracellular glucose 6-phosphate was increased from 17.6 to 99.4 μmol g^{-1} (dry cell weight) in the gene-disrupted mutant strain. The concomitant increase in the glucose 6-phosphate was accompanied by an increase in xanthan production of up to 2.23 g l^{-1} (culture medium). However, in defined medium supplemented with 0.4% glucose, the growth rate of the mutant strain was reduced to 52.9% of the wild-type level. Subsequently, when a family B ATP-dependent phosphofructokinase from *Escherichia coli* was overexpressed in the mutant strain, the growth rate was increased to 142.9%, whereas the yields of xanthan per mole of glucose remained approximately the same.

Keywords Glucose 6-phosphate dehydrogenase · Phosphofructokinase · Rate-limiting · *Xanthomonas oryzae* pv. *oryzae* · Xanthan production

S.-G. Jang · J.-Y. Cho (✉)
Department of Pharmaceutical Engineering, College of Health Science, Sangji University, Sangjidae-gil 83, Woosan-dong, Wonju-si, Gangwon-do 220-702, Korea
e-mail: jycho@sangji.ac.kr

B.-M. Lee
Microbial Genetics Division, National Institute of Agricultural Biotechnology, 225 Seodun-dong, Suwon 441-707, Korea

J.-Y. Cho
labGene Inc., Sangji University, Sangjidae-gil 83, Woosan-dong, Wonju-si, Gangwon-do 220-702, Korea

Introduction

Xanthomonas oryzae has been found to generate xanthan [6], which is an exopolysaccharide (EPS) used as a viscosifying, stabilizing, emulsifying, or gelling agent in various commercial and industrial applications [15]. Xanthan can be synthesized in the cell from sugar nucleotide precursors, and xanthan biosynthesis involves the assembly of a pentasaccharide repeating unit attached to an inner-membrane polyprenol phosphate carrier via the sequential transfer of monosaccharides from sugar nucleotides by glycosyltransferases, followed by the polymerization of the pentasaccharide repeating units and export [5].

Although xanthan biosynthesis may involve a complex network of reactions containing many possible bottlenecks, relatively little is currently known about xanthan biosynthesis in *X. oryzae*. Assuming that glucose 6-phosphate exists at the branch point of different pathways for glucose metabolism, the intracellular availability of this sugar phosphate might constitute a potential bottleneck in the process of xanthan production. However, the maximal EPS production is not limited by increasing the pool of glucose 6-phosphate in *Lactococcus lactis* [1].

It was demonstrated previously that a number of *Xanthomonas* species lack the phosphofructokinase (PFK) activity required for functional glycolysis, and exhibit an insufficient capacity of the pentose phosphate pathway for glucose catabolism [9, 17]. The results of our previous study demonstrated that the intracellular availability of glucose 6-phosphate can be increased by inactivating the phosphogluconate dehydratase gene (*edd*) involved in the Entner–Doudoroff pathway of the central carbon catabolism, and can be a rate-limiting factor in xanthan production in *X. oryzae* [7]. This finding indicated that the blockage of the central carbon catabolism may induce flux rerouting

and trigger a compensatory mechanism toward reactions supporting xanthan production, from which a new model of xanthan production may be developed. However, it remains unclear as to whether another mechanism responsible for regulating the level of glucose 6-phosphate to allow the shift between different carbon metabolisms exists; it is also still unknown whether the increased expression of the glycolytic phosphofructokinase gene (*pfkA*) can alter the flux toward xanthan biosynthesis in *X. oryzae*. In this study, we further evaluated the function of the central carbon catabolism via the inactivation of the glucose 6-phosphate dehydrogenase gene of the pentose phosphate pathway and the expression of the *pfkA* gene of the glycolytic pathway in xanthan biosynthesis in *X. oryzae*.

Materials and methods

Strains, plasmids, and growth conditions

The wild-type *X. oryzae* strain utilized in this study was *X. oryzae* KACC 10859. The wild-type and mutant *X. oryzae* cells were grown in XOL medium as described previously [16]. Growth was monitored via optical density measurements at 600 nm (OD_{600}).

The bacterial strains and plasmids constructed for this study and the oligonucleotide sequences utilized herein are provided in Table 1. Site-specific gene disruption was carried out using the nonreplicable integration vector, pK18mobsacB, which permits the marker-free disruption of the target gene [12]. In order to construct the gene-disrupted mutant strain, the pK18mobsacB integration vector harboring the internally deleted XOO2314 open reading frame (ORF) was constructed (Table 1). This recombinant plasmid was subsequently introduced into the wild-type *X. oryzae* strain via electroporation, and the gene-disrupted mutant strain was created via the method described previously by Yoon and Cho [16]. In order to construct strains overexpressing the *Escherichia coli pfkA* gene, the pKEB27 shuttle vector [10] harboring the *E. coli pfkA* coding region fused with a *X. oryzae pfk* promoter and terminator regions was also constructed (Table 1). The nucleotide sequences of the *X. oryzae* XOO2314 ORF and the *pfk* gene have been deposited in the GenBank database under the accession number AE013598. The GenBank accession number of the *E. coli* DNA sequence, *pfkA*, reported in this work is AP009048.

Enzyme assay

Xanthomonas oryzae cells were grown in XOL medium, harvested via centrifugation during the exponential phase, and washed in 100 mM Tris/HCl buffer (pH 7.5). The cells were disrupted with glass beads, and the resulting homogenate was centrifuged to obtain the crude cell-free extract. All of these treatments were conducted at 4°C. All enzyme assays were carried out at 25°C under the previously determined optimum conditions. The control contained the reaction buffers, cofactors, and the substrates, but lacked the crude cell-free extracts.

Phosphofructokinase was assayed in accordance with the methods described by Storey [13] in a reaction coupled with pyruvate kinase and lactate dehydrogenase, and measured as the change in absorbance at 340 nm due to NADH oxidation. Glucose dehydrogenase (GDH) and glucose 6-phosphate dehydrogenase (G6PDH) activity in the crude cell-free extracts were measured via spectrophotometric determination of NADPH formation at 340 nm as previously described [4, 14]. Gluconate kinase (GntK) activity in the crude cell-free extracts was measured via a coupled enzymatic assay of 6-phosphogluconate dehydrogenase (6PGD) as previously described [4]. One unit of enzyme activity was defined as the amount of enzyme required to produce 1 μmol of product per minute at 25°C.

Estimation of intracellular glucose 6-phosphate concentration

The method employed for the extraction of intracellular glucose 6-phosphate was based on the procedure of rapid inactivation of metabolism described previously by Lebloas et al. [8]. Five-milliliter culture samples were taken, frozen immediately in liquid nitrogen, and stored at −80°C. A known amount of cells was added to 2 ml of perchloric acid (25%). After three freeze–thaw cycles, the cells were removed via centrifugation. Subsequently, the extract was incubated for 8 min at 50°C prior to neutralization to pH 7–8 by 15 M KOH, and then immediately utilized in a coupled G6PDH assay to determine the intracellular glucose 6-phosphate concentrations after centrifugation. The absorption of NADPH was measured at 340 nm, and the increases in absorbance observed for the sample and for the standard were employed to calculate the concentrations of the metabolite. The dry cell weight was estimated on the basis of the correlation; 1 OD_{600} = 0.3 g (dry cell weight) l^{-1}.

RT-PCR analysis

For RT-PCR experiments, total RNA was extracted from *X. oryzae* KACC 10859 late-exponentially grown in XOL medium via the hot phenol method, and the extracted RNA was treated with DNase I. The DNase I-treated RNA samples were purified with an RNeasy® column (Qiagen). Purified DNase I-treated RNA samples were subsequently incubated for 30 min with RT primer and 200 units of reverse transcriptase at 42°C. Reverse-transcribed RNA

Table 1 Bacterial strains, plasmids, and primers used in this study

Strain, plasmid, or primer	Description or sequence (5′–3′)[a]	Source, reference, or target[b]
X. oryzae strains		
KACC 10859	Wild-type	This study
SJ3001	KACC 10859, XOO2314Δ	This study
Plasmids		
pK18mobsacB	Mobilizable vector, *oriT sacB* Km^R	[12]
pKEB27	*E. coli–X. oryzae* shuttle vector, Km^R	[10]
pSJ2004	pK18mobsacB derivative with 2,557-bp *Xba*I fragment of XOO2314 containing internal in-frame deletion of *Hin*dIII fragment generated by PCR with primer pairs 2314F1–2314R1 and 2314F2–2314R2 from *X. oryzae* KACC 10859 genomic DNA	This study
pSJ2202	pKEB27 derivative with 963-bp *Nde*I-*Hin*dIII fragment of the *E. coli pfkA* gene encompassed by 955-bp blunt-ended*Xba*I-*Nde*I fragment upstream of the *X. oryzae pfkA* coding sequence and 923-bp *Hin*dIII blunt-ended *Bam*HI fragment downstream of the *X. oryzae pfk* coding sequence	This study
Primers		
2314F1	gctctagaGCATCCAGATTGGACAGC (*Xba*I)	XOO2314 (2448841–2448858)
2314R1	cccaagcttATCGCCAGATAGCTCACG (*Hin*dIII)	XOO2314 (2450082–2450099)
2314F2	cccaagcttGGTCAAGGTACTGCGTGC (*Hin*dIII)	XOO2314 (2450535–2450552)
2314R2	gctctagaCGGTGGATGTTGACCAGG (*Xba*I)	XOO2314 (2451815–2451832)
XPFKF1	gctctagaCGCTAGTCGCAGTATCCC (*Xba*I)	*X. oryzae pfkA* (996609–996626)
XPFKR1	ggaattccatatgGGGACGGGCTCCTCA (*Nde*I)	*X. oryzae pfkA* (995672–995689)
EPFKF1	gctctagacatatgATTAAGAAAATCGGTGTG (*Nde*I)	*E. coli pfkA* (3529109–3529129)
EPFKR1	cccaagcttAATACAGTTTTTTCGCGCA (*Hin*dIII)	*E. coli pfkA* (3528167–3528187)
XPFKF2	cccaAGcTtCCCCAGTGCGGGC (*Hin*dIII)	*X. oryzae pfkA* (994398–994415)
XPFKR2	cgggatccTGTCGGGTAGCTCACTCC (*Bam*HI)	*X. oryzae pfkA* (993493–993510)
RT primer	GTTCTGGATGCCTTCGCT	*X. oryzae pfkA* (994928–994945)
PFKF	GATCAAGGTACTGGCTGC	*X. oryzae pfkA* (995556–995573)
PFKR	CCGACTTTGTCCACTACC	*X. oryzae pfkA* (994965–994982)

[a] Underlined sequences indicate restriction sites for restriction enzymes as shown in parentheses. Upper case letters refer to the sequences of bacterial genes

[b] Numerical positions on the bacterial genomes are shown in parentheses

samples were then added to the primer pairs PFKF–PFKR (Table 1), and PCR mix. PCR was routinely conducted under the following reaction conditions: 40 cycles at 95°C for 30 s, 56°C for 30 s, and 72°C for 30 s. The PCR products were subsequently analyzed via electrophoresis on 2% agarose gel.

Determination of xanthan

The wild-type and mutant *X. oryzae* strains were inoculated in XOL medium, and subsequently incubated for 48 h in a rotary shaker at 200 rpm at 28°C. The amount of xanthan in the supernatant was determined upon entry of the cells into the stationary phase of growth via the colorimetric method for the estimation of pentoses and hexoses [2], and then calculated with a standard curve constructed using a known amount of xanthan.

Results and discussion

Construction of strain with altered carbon catabolism activity

We have observed previously that the wild-type *X. oryzae* strain growing in XOL medium containing glucose as a carbon source did not exhibit PFK activity [7], as has been described for other *Xanthomonas* species [9]. This indicates that the Embden–Meyerhof–Parnas pathway of glycolysis is not functional for glucose catabolism, and G6PDH is the principal route of glucose catabolism in *X. oryzae*. Therefore, we further attempted to determine whether it is possible to influence the availability of glucose 6-phosphate to increase xanthan production by modulating G6PDH activity via the inactivation of the G6PDH gene (XOO2314 or XOO0467) in the wild-type *X. oryzae* strain, because we

Table 2 Specific activities of enzymes in the crude cell-free extracts from the wild-type and mutant strains

X. oryzae strain (plasmid)	Genotype	Specific activity (U mg of protein^{-1})[a]			
		G6PDH	GDH	GntK	PFK
KACC 10859	Wild-type	34.7	0.42	ND	ND
KACC 10859 (pSJ2202)	Wild-type	–	1.24	0.38	2.15
SJ3001	XOO2314Δ	0.69	1.44	0.39	ND
SJ3001 (pSJ2202)	XOO2314Δ	–	0.79	0.14	2.65

ND not detected

[a] The values are averages based on the results obtained with at least three independent experiments and the standard deviations were consistently <10%

have previously demonstrated that the intracellular availability of glucose 6-phosphate is a rate-limiting factor in xanthan production in *X. oryzae* [7]. The XOO2314 gene-disrupted mutant evidenced almost no residual G6PDH activity (1.99%) (Table 2), whereas the XOO0467 gene-disrupted mutant evidenced almost identical residual G6PDH activity (89.2%) relative to the wild-type strain (data not shown).

When glucose was employed as the carbon source, the XOO2314 gene-disrupted mutant strain proved capable of growth in the XOL medium at a remarkably lower growth rate than the wild-type strain (Fig. 1a). However, the yields of biomass per mole of glucose were approximately identical (112.0 vs. 123.3 g (dry wt)/mol glucose for the wild-type and mutant strain, respectively). The fact that the growth rate of the XOO2314 gene-disrupted mutant strain was reduced while the biomass yield on glucose remained unchanged indicated that *X. oryzae* may exploit two active routes for glucose catabolism for the production of 6-phosphogluconate, an intermediate of the oxidative pentose phosphate pathway, i.e., the G6PDH and GDH pathways. In order to determine the route by which glucose is converted to 6-phosphogluconate through the GDH pathway, we measured the enzyme activities of the GDH pathway enzymes, GDH and GntK, in the crude cell-free extracts from both the wild-type and mutant strains. The results are shown in Table 2. Interestingly, the activities of both GDH and GntK were increased as a result of the XOO2314 ORF gene disruption.

To assess the pattern of xanthan biosynthesis in the XOO2314 gene-disrupted mutant strain, xanthan production was determined in the mutant strain grown in the XOL medium supplemented with 0.4% glucose (Table 3). The XOO2314 gene-disrupted mutant strain produced significantly larger amounts of xanthan than the wild-type strain did. One explanation for the altered phenotype of the XOO2314 gene-disrupted mutant strain could be that the reduced G6PDH activity resulted in an accumulation of glucose 6-phosphate, which has previously been shown to be limited in xanthan production. Indeed, the concentrations of glucose 6-phosphate were found to be increased to 99.4 μmol g^{-1} (dry cell weight) in the XOO2314 gene-disrupted mutant strain, as compared to the 17.6 μmol g^{-1} (dry cell weight) measured in the wild-type strain.

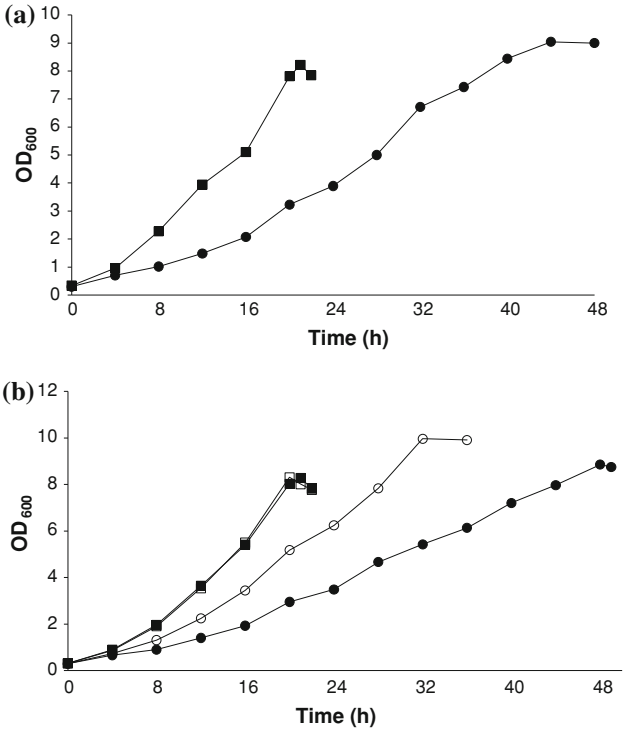

Fig. 1 Growth of the *X. oryzae* wild-type and mutant strains in XOL medium supplemented with 0.4% (w/v) glucose. **a** *Filled square*, wild-type; *filled circle*, the XOO2314 gene-disrupted mutant. **b** *Filled square*, wild-type harboring the plasmid pKEB27; *open square*, wild-type harboring the plasmid pSJ2202; *filled circle*, the XOO2314 gene-disrupted mutant harboring the plasmid pKEB27; *open circle*, the XOO2314 gene-disrupted mutant harboring the plasmid pSJ2202. OD_{600}, optical density at 600 nm. Three independent extractions were conducted for each growth phase

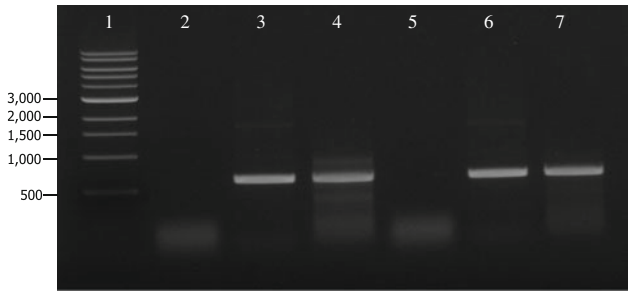

Fig. 2 RT-PCR analysis of the *pfk* gene transcript generated by the wild-type (*lanes 2–4*) and XOO2314 gene-disrupted mutant (*lanes 5–7*) strains. For the positive control, the presence of the expected amplicon when genomic DNA was included in the control sample demonstrated the reliability of the primer pair, PFKF–PFKR (*lanes 2* and *5*). For the negative control, no amplicon was detected when total RNA that was treated with DNase I but was not reverse-transcribed and served as the template, ensuring that residual genomic DNA had not contaminated the total RNA preparation (*lanes 3* and *6*). The cDNA fraction obtained with the RT primer was used for subsequent PCR reactions with PFKF–PFKR primer pair (*lanes 4* and *7*). DNA size markers in base pairs are indicated (*lane 1*)

Complementing the reduced activity of carbon catabolism of the mutant strain

Although no PFK activity was observed in the wild-type and XOO2314 gene-disrupted mutant strain growing in the XOL medium containing glucose as a carbon source (Table 2), *pfk*-specific transcription was detected via RT-PCR analysis (Fig. 2). This uncoupled relation between gene transcript abundance and enzyme activity may be attributable to the presence of allosteric inhibitors of ATP-dependent PFKs [3]. We therefore attempted to restore the PFK activity by complementation. The XOO2314 gene-disrupted mutant strain was transformed with pSJ2202, which harbors the *E. coli pfkA* gene transcribed from the *X. oryzae pfk* promoter. As shown in Table 2, successful expression of the *E. coli* PFK in the mutant strain harboring the pSJ2202 plasmid was indicated by measuring the PFK activity in the crude cell-free extracts using a coupled enzyme assay. Although the specific activity of PFK in the XOO2314 gene-disrupted mutant strain harboring the pSJ2202 plasmid was found to be low compared with the PFK activity measured in *E. coli* [11], the strain harboring the pSJ2202 plasmid evidenced a significantly higher growth rate on glucose relative to the control strain (Table 3; Fig. 1b). Notably, the increased expression of the PFK activity in the XOO2314 gene-disrupted mutant strain did not affect the xanthan production level as compared with the control strain (Table 3). In addition, the effects of increased expression of the PFK activity on the enzyme activities of GDH pathway enzymes and the glucose 6-phosphate levels were analyzed. The higher activity of PFK in the XOO2314 gene-disrupted mutant strain resulted in the reduced levels of glucose 6-phosphate [99.4 versus 54.9 μmol g^{-1} (dry cell weight) for the XOO2314 gene-disrupted mutant strain and the mutant strain harboring pSJ2202, respectively] and GDH pathway enzyme activities (Table 3). This is contrary to what was observed for the wild-type strain. Higher activities of GDH pathway enzymes were observed in the wild-type strain with the higher activity of PFK (Table 3), while the levels of glucose 6-phosphate remained relatively unchanged [17.6 versus 21.5 μmol g^{-1} (dry cell weight) for the wild-type strain and the wild-type strain harboring pSJ2202, respectively].

The findings of this study indicated that different G6PDH activity levels affected the concentration of glucose 6-phosphate, and that an increased concentration of glucose 6-phosphate exerted a significant effect on xanthan production when the cells were cultivated on glucose. The mutant strain was still able to grow on glucose using the central carbon metabolism, including the pentose phosphate pathway and the Entner–Doudoroff pathway; this may be because the availability of the GDH pathway induced more activity in the mutant strain with regard to the formation of 6-phosphogluconate from glucose. An additional explanation for the altered phenotype of the mutant strain might be that the limited contribution of PFK to glucose catabolism in aerobically cultivated cells resulted in increased channeling

Table 3 Effects of modulating G6PDH activity of the *X. oryzae* wild-type strain on growth and xanthan production

X. oryzae strain	Plasmid	Growth (h^{-1})[a]	Xanthan concentration (g l^{-1})	Xanthan yield (g g^{-1})
KACC 10859	pKEB27	0.202	1.40	0.35
KACC 10859	pSJ2202	0.202	1.41	0.35
SJ3001	pKEB27	0.107	2.48	0.62
SJ3001	pSJ2202	0.153	2.39	0.59

ND not detected

The values are averages based on the results obtained with at least three independent experiments and the standard deviations were consistently <10%

[a] The rates given are maximal specific growth rate observed during the exponential phase

of carbon flow toward xanthan biosynthesis. As a consequence, the carbon flux may be redistributed at the branch point of glucose 6-phosphate toward xanthan biosynthesis relative to the wild-type strain. Apparently, under conditions in which the glycolytic flux is increased due to the expression of *E. coli* PFK, the growth rate of the mutant strain increases significantly. Another consequence of the slightly elevated expression of *E. coli* PFK activity in the mutant strain is a constant level of xanthan yield on glucose (gram per gram) with the reduced levels of glucose 6-phosphate and GDH pathway enzyme activities, which suggests a mechanism by which the cells can balance glucose catabolism for xanthan production. The fact that an elevated expression of *E. coli* PFK activity in the wild-type strain resulted in the constant level of glucose 6-phosphate with no significant changes in growth and xanthan production, whereas the GDH pathway enzyme activities were increased, is likely to reflect the rigidity of the glucose 6-phosphate branch point. To clarify whether the glucose 6-phosphate branch point is indeed strongly rigid for glucose catabolism, it would be necessary to compare the expected consequences that perturbation strongly increases PFK activity with the observed results.

The results presented in this work emphasize the importance of targeting the central carbon metabolism to enhance xanthan biosynthesis, primarily by evaluating the role of glucose 6-phosphate at the branching point between glucose catabolism and anabolism in *X. oryzae*. However, further investigation will be necessary to determine whether glucose 6-phosphate is relevant to the control of glucose catabolism and anabolism.

Acknowledgments This research was supported by the Agenda Program (Grant PJ006631042011) funded by the Rural Development Administration, Republic of Korea, and in part by the Sangji University Research Fund 2010. *lab*GENE Inc. was supported by a grant from the Gangwon Technopark.

References

1. Boels IC, Kleerebezem M, de Vos WM (2003) Engineering of carbon distribution between glycolysis and exopolysaccharide biosynthesis in *Lactococcus lactis*. Appl Environ Microbiol 69:1129–1135
2. DuBois M, Gilles KA, Hamilton JK, Rebers PA, Smith F (1956) Colorimetric method for determination of sugars and related substances. Anal Chem 28:350–356
3. Fenton AW, Paricharttanakul NM, Reinhart GD (2003) Identification of substrate contact residues important for the allosteric regulation of phosphofructokinase from *Escherichia coli*. Biochemistry 42:6453–6459
4. Frunzke J, Engels V, Hasenbein S, Gätgens C, Bott M (2008) Co-ordinated regulation of gluconate catabolism and glucose uptake in *Corynebacterium glutamicum* by two functionally equivalent transcriptional regulators, GntR1 and GntR2. Mol Microbiol 67:305–322
5. Ielpi L, Couso RO, Dankert MA (1993) Sequential assembly and polymerization of the polyprenol-linked pentasaccharide repeating unit of the xanthan polysaccharide in *Xanthomonas campestris*. J Bacteriol 175:2490–2500
6. Kim S-Y, Kim J-G, Lee B-M, Cho J-Y (2009) Mutational analysis of the *gum* gene cluster required for xanthan biosynthesis in *Xanthomonas oryzae* pv *oryzae*. Biotechnol Lett 31:265–270
7. Kim S-Y, Lee B-M, Cho J-Y (2010) Relationship between glucose catabolism and xanthan production in *Xanthomonas oryzae* pv. *oryzae*. Biotechnol Lett 32:527–531
8. Lebloas P, Guilbert N, Loubiere P, Lindley ND (1993) Growth inhibition and pyruvate overflow during glucose catabolism by *Eubacterium limosum* is related to a limited capacity to reassimilate CO_2 by the acetyl-CoA pathway. J Gen Microbiol 139:1861–1868
9. Letisse F, Chevallereau P, Simon J-L, Lindley N (2002) The influence of metabolic network structures and energy requirements on xanthan gum yields. J Biotechnol 99:307–317
10. Makino S, Sugio A, White F, Bogdanove AJ (2006) Inhibition of resistance gene-mediated defense in rice by *Xanthomonas oryzae* pv. *oryzicola*. Mol Plant Microbe Interact 19:240–249
11. Ogawa T, Mori H, Tomita M, Yoshino M (2007) Inhibitory effect of phosphoenolpyruvate on glycolytic enzymes in *Escherichia coli*. Res Microbiol 158:159–163
12. Schäfer A, Tauch A, Jäger W, Kalinowski J, Thierbach G, Pühler A (1994) Small mobilizable multi-purpose cloning vectors derived from the *Escherichia coli* plasmids pK18 and pK19: selection of defined deletions in the chromosome of *Corynebacterium glutamicum*. Gene 145:69–73
13. Storey KB (1976) Purification and properties of adductor muscle phosphofructokinase from the oyster, *Crassostrea virginica*. The aerobic/anaerobic transition: role of arginine phosphate in enzyme control. Eur J Biochem 70:331–337
14. Sugimoto S-I, Shiio I (1987) Regulation of glucose-6-phosphate dehydrogenase in *Brevibacterium flavum*. Agric Biol Chem 51:101–108
15. Sutherland IW (1998) Novel and established applications of microbial polysaccharides. Trends Biotechnol 16:41–46
16. Yoon K-H, Cho J-Y (2007) Transcriptional analysis of the *gum* gene cluster from *Xanthomonas oryzae* pathovar *oryzae*. Biotechnol Lett 29:95–103
17. Zagallo AC, Wang CH (1967) Comparative glucose catabolism of Xanthomonas species. J Bacteriol 93:970–975